Criteria for fast and selective α precipitation at β grain boundaries in Ti-alloys Consequence for in-service microstructures

Tao Liu, Lionel Germain, Julien Teixeira, Elisabeth Aeby-Gautier, Nathalie Gey

Criteria for fast and selective α precipitation at β grain boundaries in Ti-alloys

Consequence for in-service microstructures

Tao Liu[1,2], Lionel Germain[1,2], Julien Teixeira[2,3], Elisabeth Aeby-Gautier[2,3], Nathalie Gey[1,2,*]

[1]Laboratoire d'Etude des Microstructures et de Mécanique des Matériaux, CNRS, Université de Lorraine; Ile du Saulcy; Metz, F-57045 CEDEX 1, France

[2]Laboratory of Excellence for Design of Alloy Metals for Low-mass Structures ('DAMAS' Labex), University de Lorraine, France

[3]Institut Jean Lamour, CNRS, Université de Lorraine; Parc de Saurupt; Nancy, CS 50840 F-54011 CEDEX, France

*nathalie.gey@univ-lorraine.fr

Abstract

The potential for β grain boundaries (GBs) to give rise to large Widmanstätten colonies was determined through the observation of a large amount of precipitates at β GBs in a β-metastable titanium alloy using electron backscatter imaging and diffraction. The most critical boundaries are those which transform early and where a type of Variant Selection (VS) called double Burgers VS occurs. This mechanisms take place at 'special' β boundaries misoriented so that an α precipitate can be related to both grains through the Burgers relation. It was shown that the most critical GBs have a disorientation at an angle of less than 10° from 49.5°/<110> or 60°/<110>. A simulation study allowed those boundaries to be quantifed in crystallographic textures typical of industrial products. Those texture have then been discussed as a function of their potential to form large Widmanstätten colonies.

1. Introduction

In-service fatigue performance of titanium alloys decreases in the presence of large α regions with a single orientation which may act as fatal crack initiation sites [1-4]. Some of these large regions correspond to Widmanstätten colonies that are nucleated on both side of a grain boundary (GB). In general, the colonies inherit their crystallographic orientation from an allotriomorph α layer ($α_{GB}$) decorating the β GBs and acting as a precursor. The $α_{GB}$ nucleates in Burgers Orientation Relationship (BOR) (i.e.

$$\{110\}_\beta // \{0001\}_\beta \ and \ \langle 1\bar{1}1 \rangle_\beta // \langle 11\bar{2}0 \rangle$$

) with at least one β grain. According to the BOR, each β grain can generate a maximum of 12 α variants. One speaks of Variant Selection (VS) when a mechanism favors the precipitation of some variants. Two mechanisms drive the formation of large Widmanstätten colonies: early $α_{GB}$ precipitation and VS [5]. As noticed by Salib et al. [5], the first $α_{GB}$ precipitates emit their colonies earlier and this leaves little room for late precipitates to emit colonies. A VS mechanism called 'double BOR' plays also an important role in large colonies development. It was observed that a variant in BOR with both β grains is preferencially precipitated. As a result, two colonies with the same orientation are emitted in the two adjacent β grains, and so form anormally large crystallographic domains [2,5]. This mechanism only applies when neighboring β grains have one of the following four 'special' disorientations: Type I - 10.5°/<110>, Type II - 49.5°/<110>, Type III - 60°/<110>, Type IV - 60°/<111> [6]. Even if double BOR VS is well documented in Ti-alloys [5-8], the frequency of its occurrence as a function of the texture (i.e of the processing route) was never studied. Additionnaly, a better understanding of the parameters controlling the $α_{GB}$ precipitation may help to improve the in-service properties.

In this work, we present a statistical study of the early precipitation and VS at β GBs. As a result, β GBs were classified as a function of their potential to produce large colonies. The statistical distribution of the 'special' boundaries are then quantified in different β textures of industrial products to evaluate if some textures are preferable to avoid large colonies.

2. Material and experiments

A Ti-17 β-metastable alloy (5%Al, 4%Cr, 4%Mo, 2%Sn, 2%Zr (in w%), 1200ppm O and Ti-balance) was used to study the early stage of $\beta \rightarrow \alpha_{GB}$ transformation. The β grains were equiaxed with an average diameter of 200 μm after a solution treatment at 920°C for 30 minutes (β transus T_β = 880°C). From 920°C, the sample was helium quenched to the transformation temperature of 800°C and maintained 200s so that the α transformation was restricted to the firstly formed α_{GB} [7]. In this context, we focus on the β GBs first transformed. α_{GB} precipitation was assessed as a function of the crystallographic characteristics of GBs. For this purpose, EBSD orientation maps were acquired in a ZEISS Auriga focused ion beam scanning electron microscope (FIB-SEM) equipped with a Bruker QUANTAX EBSD acquisition system. The total scanned area of 8 × 0.8mm² (step size: 1μm) covered more than 1000 β GBs. Since the coarse step size used did not allow the α precipitates to be indexed, the β GBs were further imaged with the backscatter electron detector (BSE-D) to identify the presence of α_{GB} precipitation and assess their morphology. The EBSD maps were automatically analyzed with our home-made software DECRYPT (Direct Evaluation of CRYstallorgaphic Phase Transformation). This software is dedicated to analyzing the orientation data inherited by OR-based phase transformations. For each GB, the following entries were inventoried: β GB disorientation angle and axis, closest 'special' GB type (I to IV) and disorientation angle to the closest 'special' GB (called $\theta_{2\text{-}BOR}$). The presence of a precipitate based on the BSE observation was manually added to the data. To study the double-BOR VS, 74 α precipitates were finely scanned with EBSD using a step size of 0.25μm. In this case, DECRYPT inventoried also if double-BOR VS was respected.

3. Results and discussion

3.1. Precipitation per 'special' GB type

The early decorated β GBs are considered as preferential sites for nucleation and growth of α_{GB} layers. This study gives a better understanding of where precipiatation occurs first. After 200s at 800°C, 16.2% (in length) of the 1129 GBs identified in the large-area EBSD map were decorated by α_{GB} precipitates. They were almost fully decorated by α_{GB} layers with a single orientation of about 1μm in thickness.

Fig. 1 presents the analysis of the β GB precipitation as a function of the $\theta_{2\text{-}BOR}$ angle. The lower this angle, the closer the GB is to the 'special' GBs. A disorientation threshold of 15° is applied to separate the low angle GBs (LAGB) from the high angle GBs (HAGB). For HAGB, the transformed fraction is highly dependent of the $\theta_{2\text{-}BOR}$ angle. It reaches about 70% when $\theta_{2\text{-}BOR}$ is below 4° and steadily decreases until it reaches the average value of 20% at $\theta_{2\text{-}BOR} < 14°$. The decoration rate of LAGB is low (4%) and is not sensitive to the $\theta_{2\text{-}BOR}$ angle.
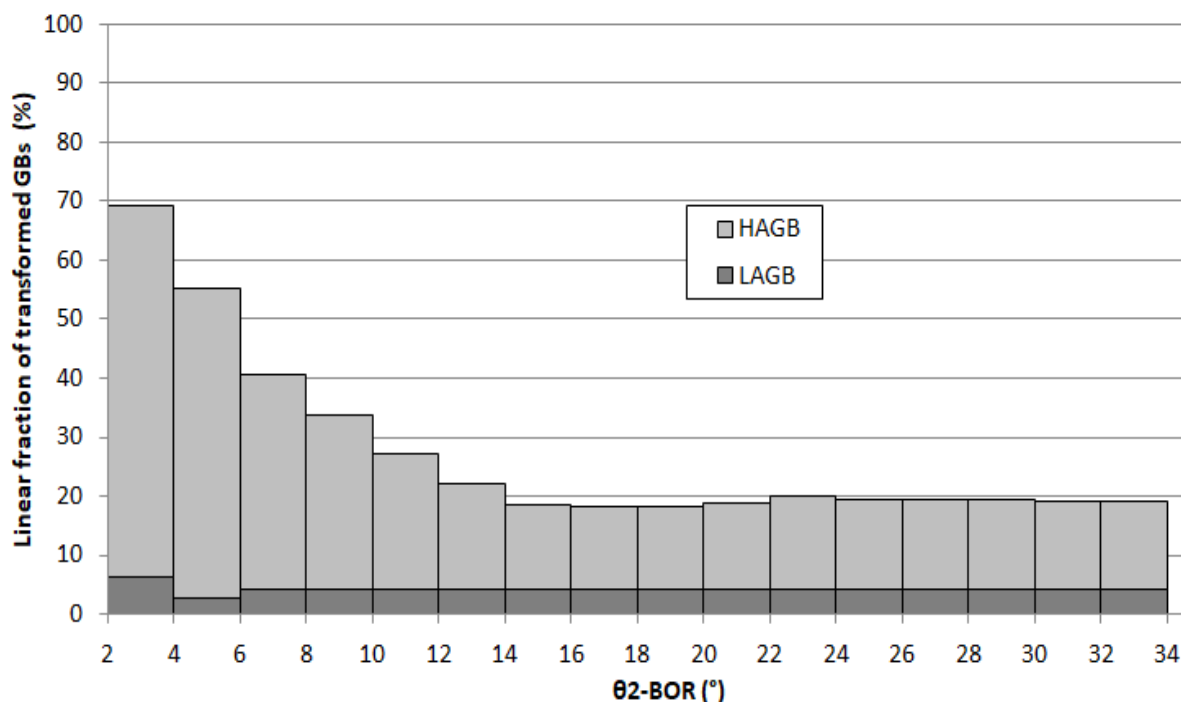

Fig. 1. Fraction of transformed boundaries as a function the disorientation to the closest 'special' boundary.

The boundary type also influences the precipitation. Type II and III GBs have the highest decoration rate. It reaches 100% at $\theta_{2\text{-BOR}} < 4°$ and is close to 50% for $\theta_{2\text{-BOR}} < 10°$ compared to 20% for all HAGBs. All Type I GBs correspond to LAGBs and their average decoration rate of 4% is relatively independent of $\theta_{2\text{-BOR}}$. The decoration rate of Type IV GBs is around the average but tends to increase with increasing $\theta_{2\text{-BOR}}$. Fig. 2 shows representative examples of Type I and II GBs at the early stage of transformation: Type I GBs clearly show no α_{GB} precipitation (Fig. 2a) whereas Type II GB is fully decorated with an α_{GB} layer and has even started to emit α Widmanstätten colonies (Fig. 2b). Type II and III GBs ($\theta_{2\text{-BOR}} < 10°$) play an important role in precipitation since they represent 40% of all transformed GBs (13% of the total GBs). The low precipitation rate of Type I, IV and LAGBs can be explained by their low GB energy. However, the much higher precipitation rate of Type II and III GBs relative to other HAGBs cannot be explained only by GB energy. Indeed, all HAGBs (special GBs included) have almost the same energy. In this case, VS has to be considered (see next section).
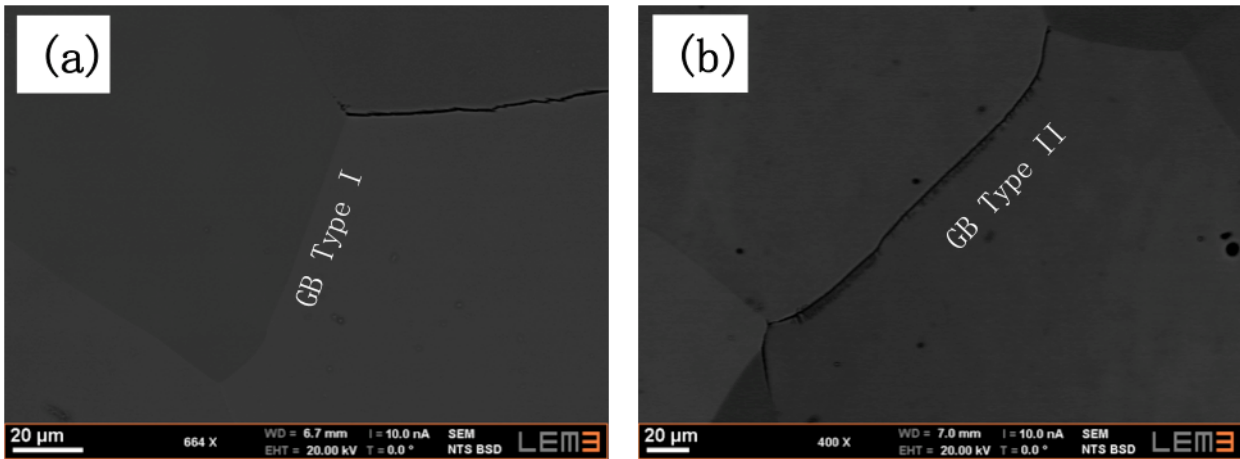

Fig.2. (a) Type I GB showing no α_{GB} layer and (b) Type II GB fully decorated with an α_G layer and even early emission of α Widmanstätten colonies.

3.2. VS per 'special' GB type

The goal of this section is to assess the conditions in which the double-BOR mechanism is relevant. Among the 180 GBs having a precipitate, 74 were chosen for VS assessement and finely scanned to measure their α_{GB} orientation. The individual measurements are plotted per boundary types in Fig. 3. A majority (55%) were 'special' GBs with $\theta_{2\text{-BOR}} < 10°$: 2 Type I, 26 Type II, 10 Type III and 3 Type IV. All of them respected the double BOR VS criterion. 9 out of the 74 transformed GBs have a $\theta_{2\text{-BOR}}$ between 10° and 16° with a VS remaining higher than average. However, it shall be noticed that sampling was sparse in this range. Beyond 16° among the remaining 24 GBs, only 7% respect the double-BOR criterion. This value shall be compared to the occurrence of the VS when variants are randomly selected (1/12 = 8.33%). Those results are in agreement with the results of Shi et al. who peformed a similar study on a smaller dataset [8].
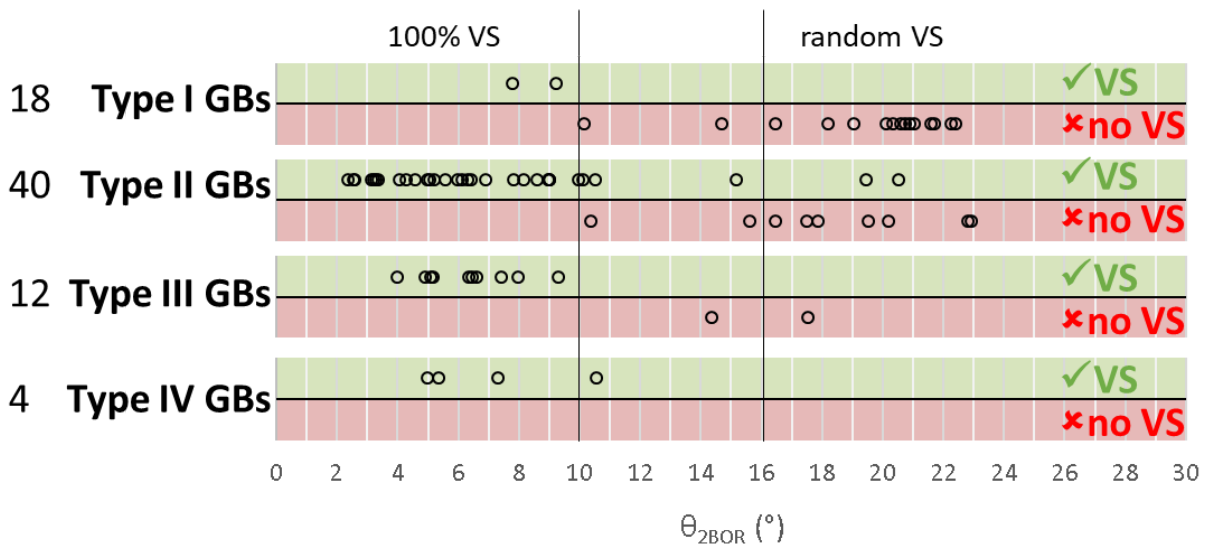
Fig. 3. VS per boundary types and $\theta_{2\text{-BOR}}$ for the 74 finely scanned α_{GBs}.

This observation can be explained considering interface energies. During nucleation and growth, each β GB is progressively replaced by two α_{GB}/β interfaces. At short incubation time, nucleation occurs where the energy balance is the most favourable, i.e. where β GBs have a high energy and α_{GB}/β interfaces, a low energy. Semi-coherent α_{GB}/β interfaces have an energy around 0.05 J/m² (such as in Widmanstätten colonies) whereas incoherent ones are around 0.4 J/m² [9]. Furuhara et al. found that the α_{GB} in BOR with both grains is semi-coherent with both β grains even if a small disorientation around one of the grains existed [10]. Therefore, precipitates respecting the double-BOR mechanisms are energetically favored. This explains that all precipitates with $\theta_{2\text{-BOR}}$ <10° respect this criterion and that Type II and III GBs have a decoration rate higher than random HAGBs.

3.3 Consequences for the in-service microstructure

The large crystallographic domains like double colonies may be limited by tailoring the processing conditions. In this work, we have demonstrated that Type II and III GBs are the most critical GBs since they form early and always respect the double BOR VS criterion. Type IV GBs are second in criticality. They respect the VS criterion but the emitted double colonies at these boundaries would be smaller since their α_{GB} formation is delayed. Type I GBs are least critical because they have a delayed formation of α_{GB}.

The distribution of prior β GBs in a material is inherited from its thermo-mechanical history and in particular its β texture and microtexture. The distribution of special GBs was quantified for typical textures encountered in titanium products using a Monte-carlo approach. The orientation of the grains were modeled as summarized in Table 1. Some scatter was added in the form of a rotation around a random axis by an angle respecting a gaussian distribution with a half-width amplitude of 10°. The GB distribution was obtained by drawing 100 000 random couples of β orientations for each texture. For each GB, both the closest boundary type and the $\theta_{2\text{-BOR}}$ deviation were calculated. The grains with $\theta_{2\text{-BOR}}$ < 10° were considered special and their frequency was plotted in Fig. 4. To evaluate the criticality of different textures in terms of double-BOR VS, the boundary fraction of Type II, III and IV were added together under the "Sum" histogram. They are referred to as critical GBs in the following.

Table 1. Different pure textures modeled in this work. Noise was introduced in the form of a rotation around a random axis and angle distributed according to a Gaussian function with halfwith at 10°.

Texture	Typically encountered in	Euler angles (rad)
Random	-	$\phi_1 = 0..2\pi$, $\Phi = \arccos(0..1)$, $\phi_2 = 0.. 2\pi$
<001> fiber	Solidification or uniaxial compression + annealing	$\phi_1 = 0..2\pi$, $\Phi = 0$, $\phi_2 = 0$
<111> fiber	Uniaxial compression at high strainrate	$\phi_1 = 0..2\pi$, $\Phi = \arccos(\sqrt{3}/3)$, $\phi_2 = \pi/4$
Hot Rolling	Hot rolled plates and sheets	10% of $\phi_1 = \pi/4$, $\Phi = 0$, $\phi_2 = 0$ 35% of <111> fiber 55% of $\phi_1 = 0$, $\Phi = \text{acos}(\pm(\sqrt{6}/3..\sqrt{3}/3))$, $\phi_2 = \pi/4$
<001> + <111> fibers	Uniaxial compression	50% of <001> fiber 50% of <111> fiber
<110> fiber	Drawing, extrusion or cogging (in the center).	$\phi_1 = 0..2\pi$, $\Phi = \pi/4$, $\phi_2 = 0$

In Fig. 4, the random texture is regarded as a reference and the other textures are ranked by increasing critical GBs fraction. The fraction of critical GBs in the random texture is 18%. This is not the lowest fraction of critical GBs. The lowest fraction is encountered in the <001> fiber (0.1%). This is because it is not possible to exceed a 45° rotation around the <001> axis and the lowest disorientation angle of the critical GBs is 49.5° (Type II). In the <111> fiber, the fraction of critical GBs is still below that of the random level (15.5%) and is mainly composed of Type IV GBs which are less critical.

The last three textures have critical GB fraction above random level. The hot rolling texture has a fraction just exceeding that of the random texture (22.5%). The <001>+<111> fibers have a fraction of 26.5%. This fraction is well above that of the two fibers taken separately. This means that a large fraction of critical GB are formed when a <111> grain is next to a <001> grain. The <011> fiber texture has the highest fraction of critical GBs (37%). This is because all the 'special' boundaries correspond to the disorientation around a <110> axis (even Type IV GBs which can be written as 70.5°/<110>).

It should be noted that the Monte-carlo approach, used in this study, modeled an uncorrelated disorientation distribution function (i.e. independant of the localization). In a correlated distribution function, real neighbor pairs are considered. In practice, two differences may be observed if a correlated disorientation distribution function would be used: the fraction of LAGB would be higher and successive heating and cooling may produce more 'special' GBs by a reverse double BOR VS as explained in [11]. The presence of a higher fraction of LAGB would decrease the fraction of HAGB and consequently those of 'special' GBs. Inversely, the reverse double BOR VS should increase the ratio 'special' GBs to HAGB. If those two effect counter balance, then the present analysis should give a good approximation of the fraction of critical GBs. This simulation study revealed that sharp texture can present both more or less special GBs than a random texture. The worst by far being the texture formed by extrusion or cogging.

The second aspect that may be adjusted is the cooling after forging. In fact, it is well established that at higher undercooling the transformation kinetics is accelerated by either a more rapid nucleation and growth kinetics of a_{GB} layers allowing the simultaneous growth of several colonies or by the nucleation of α platelets on intragranular nucleation sites [12]. The formation of large double colonies could be limited or avoided by a more efficient cooling rate favoring a rapid nucleation and growth on most HAGBs followed by the growth of numerous colonies and/or by the nucleation and growth of intragranular α platelets. The possibility to control the effect of the cooling rate, particularly in large parts, will strongly depend on the chemical composition of the alloy, its quenchability and the thermo-mechanical treatment before the cooling.
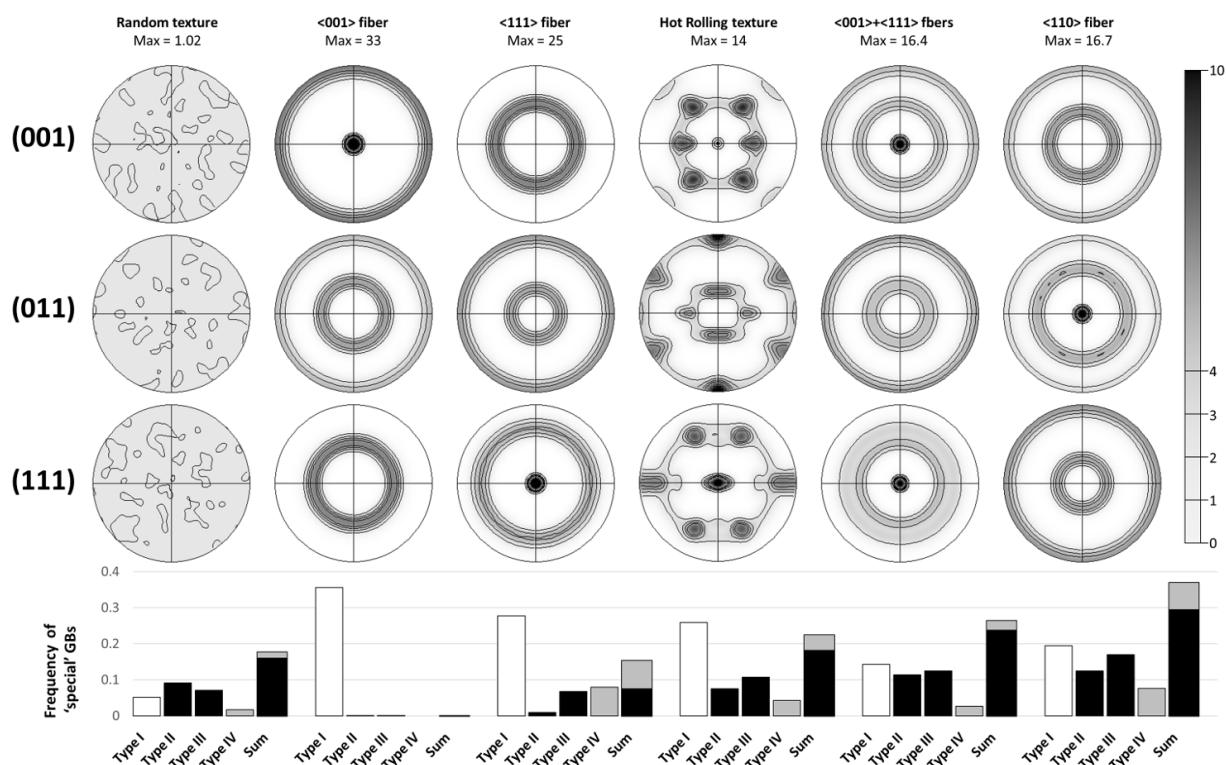

Fig.4.
Frequency of special GBs for typical textures according to the Monte-Carlo approach.

4. Conclusions

This work offers a deep analysis of early GBs decoration in a β-metastable titanium alloy to identify the probability of a GB to transform early according to a disorientation criterion and to predict the orientation of the $α_{GB}$ layers. The $α_{GB}$ layers precipitate on HAGBs with a much higher frequency than on LAGBs at the early stage of transformation. The transformation frequency

varies largely according to the type of special GBs: special HAGBs disoriented close to 49.5°/<110> or 60°/<110> have a transformation frequency close to 100%. Special GBs disorientated by 60°/<111> have no advantage for fast transformation over random HAGB and the special LAGBs disorientated by 10.5°/<110> do not transform early at all.

The α_{GB} layers observed at 'special' GBs ($\theta_{2\text{-BOR}}$ < 10°) always respect the double-BOR VS criterion. A progressive drop in VS frequency is observed beyond 10°, and it reaches the level of no VS (8%) at $\theta_{2\text{-BOR}}$ > 16°. The evolution of the VS frequency with the $\theta_{2\text{-BOR}}$ deviation is essential to predict the occurrence of this mechanism according to a given β microtexture and the transformation progress. It explains the main differences reported in the literature.

From this research, it is possible to evaluate the frequency of critical α_{GB} precursors according to the β microtexture and phase transformation path. It was shown that the <001> fibre texture limit the frequency of critical GBs. The random texture (often considered as optimal because of its isotropy) is not the one with the lowest fraction of critical GBs. The texture having the highest fraction of critical GBs is the <110> fiber which formed during extrusion or cogging.

5. Acknowledgements

6. References

1. R. Whittaker, K. Fox, A. Walker, Mater Sci Technol 26 (2010) 676-684.
2. G. Lutjering, Mater Sci Eng A 243 (1998) 32-45.
3. G.R. Yoder, F.H. Froes, D. Eylon, Metall Trans A 15 (1984) 183-197.
4. W.H. Miller, R.T. Chen, E.A. Starke, Metall Trans A 18 (1987) 1451-1468.
5. M. Salib, J. Teixeira, L. Germain, E. Lamielle, N. Gey, E. Aeby-Gautier, Acta Mater. 61 (2013) 3758-3768.
6. L. Germain, N. Gey, M. Humbert, Ultramicroscopy 107 (2007) 1129-1135.
7. T. Liu, L. Germain, J. Teixeira, E. Aeby-Gautier, N. Gey. Acta Mater. 141 (2017) 97-108.
8. R. Shi, V. Dixit, H.L. Fraser, Y. Wang. Acta Mater. 75 (2014) 156-166.
9. S. Zherebtsov, G.Salishchev, S. Lee Semiatin. Philosophical Magazine Letters 90 (2010) 903-914.
10. T. Furuhara, S. Takagi, H. Watanabe, T. Maki, Metall Trans A 27 (1996) 1635-1646.
11. J. Romero, M. Preuss, J. Quinta da Fonseca, Acta Mater. 57 (2009) 5501–5511.
12. E. Aeby-Gautier, F. Bruneseaux, J. Da Costa Teixeira, B. Appolaire, G. Geandier, S. Denis, JOM 59 (2007) 54-58.